

**Threshold resummation for the inclusive-hadron cross section in  $pp$  collisions**Daniel de Florian<sup>1</sup> and Werner Vogelsang<sup>2</sup><sup>1</sup>*Departamento de Física, FCEYN, Universidad de Buenos Aires, (1428) Pabellón 1 Ciudad Universitaria, Capital Federal, Argentina*<sup>2</sup>*Physics Department and RIKEN-BNL Research Center, Brookhaven National Laboratory, Upton, New York 11973, USA*

(Received 28 January 2005; published 6 June 2005)

We study the resummation of large logarithmic perturbative corrections to the partonic cross sections relevant for the process  $pp \rightarrow hX$  at high transverse momentum of the hadron  $h$ . These corrections arise near the threshold for the partonic reaction and are associated with soft-gluon emission. We perform the resummation to next-to-leading logarithmic accuracy. We present numerical results for the fixed-target regime and find enhancements over the next-to-leading order cross section, which significantly improve the agreement between theoretical predictions and data. We also apply the resummation for Relativistic Heavy-Ion Collider kinematics and find that subleading terms appear to play a rather important role here.

DOI: 10.1103/PhysRevD.71.114004

PACS numbers: 12.38.Cy, 13.85.Ni

**I. INTRODUCTION**

Cross sections for single-inclusive hadron production in hadronic collisions,  $H_1 H_2 \rightarrow hX$ , play an important role in QCD. At sufficiently large hadron transverse momentum  $p_T$ , one expects that QCD perturbation theory can be used to derive predictions for the reaction. Since high  $p_T$  implies large momentum transfer, the cross section may be factorized at leading power in  $p_T$  into convolutions of long-distance pieces representing the structure of the initial hadrons and the fragmentation of a final-state quark or gluon into the observed hadron, and parts that are short-distance and describe the hard interactions of the partons. The long-distance contributions are universal, i.e., they are the same in any inelastic reaction, whereas the short-distance pieces depend only on the large scales related to the large momentum transfer in the overall reaction and, therefore, can be evaluated using QCD perturbation theory. Because of this, and because of the fact that single-inclusive hadrons (e.g., pions) are rather straightforward observables in experiment, cross sections for  $H_1 H_2 \rightarrow hX$  offer a variety of important insights into strong interaction dynamics.

If the long-distance pieces, parton distribution functions and fragmentation functions, are known from other processes, especially deeply-inelastic scattering and hadron production in  $e^+e^-$  annihilation, one may test the perturbative framework outlined above. In particular, one may examine the relevance of higher orders in the perturbative expansion. Any discrepancies between the predictions and experimental data may also provide information about power-suppressed contributions to the cross section.

Alternatively, one may also gain information about fragmentation functions. For example,  $e^+e^-$  annihilation is mostly sensitive to quark-to-hadron fragmentation functions, whereas data from hadronic collisions may also provide information on gluon fragmentation. In addition, the reaction  $H_1 H_2 \rightarrow hX$  may be used to probe the structure of the initial hadrons. Of particular relevance here are spin effects, associated with polarized initial protons. At

the BNL Relativistic Heavy-Ion Collider (RHIC), one measures spin asymmetries in polarized  $pp \rightarrow hX$  scattering, in order to investigate the spin structure of the nucleon. Finally, high- $p_T$  hadrons are also important probes of strongly interacting matter in a high-energy nuclear environment, as generated by heavy-ion collisions. Here, hadron production in proton-proton collisions provides an important baseline for the study of nuclear dynamics.

Whatever the uses of processes  $H_1 H_2 \rightarrow hX$ , a central piece is in each case the perturbative partonic hard scattering and our ability to reliably evaluate it. Lowest-order (LO) calculations of the partonic short-distance cross sections were performed a long time ago [1], and later improved when the next-to-leading order (NLO) corrections were computed [2–4]. On the experimental side, an extensive data set on high- $p_T$  single-inclusive hadron data has been collected, both from scattering off fixed targets and from colliders at much higher energies. Detailed comparisons of NLO calculations with the experimental data have been carried out recently in [5–8]. They show the overall trend that NLO theory significantly underpredicts the cross section data at fixed-target energies, but yields a good description [8–10] of the collider data.

In the present paper, we further improve the theoretical calculations by implementing the all-order resummation of large logarithmic corrections to the partonic cross sections. At partonic threshold, when the initial partons have just enough energy to produce a high-transverse momentum parton (which subsequently fragments into the observed hadron) and a massless recoiling jet, the phase space available for gluon bremsstrahlung vanishes, resulting in large logarithmic corrections to the partonic cross section. To be more specific, if we consider the cross section as a function of the hadron transverse momentum  $p_T$ , integrated over all hadron rapidity, the partonic threshold is reached when  $\sqrt{\hat{s}} = 2\hat{p}_T$ , where  $\sqrt{\hat{s}}$  is the partonic center-of-mass (c.m.) energy, and  $\hat{p}_T = p_T/z$  is the transverse momentum of the produced parton fragmenting into the hadron, the latter taking the fraction  $z$  of the parton mo-

mentum. Defining  $\hat{x}_T \equiv 2\hat{p}_T/\sqrt{\hat{s}}$ , the leading large contributions near threshold arise as  $\alpha_s^k \ln^{2k}(1 - \hat{x}_T^2)$  at the  $k$ th order in perturbation theory, where  $\alpha_s$  is the strong coupling. Sufficiently close to threshold, the perturbative series will be only useful if such terms are taken into account to all orders in  $\alpha_s$ , which is what is achieved by threshold resummation [11–13]. This resummation has been derived for a number of cases of interest, to next-to-leading logarithmic (NLL) order. As far as processes with similar kinematics are concerned, it has been investigated for high- $p_T$  prompt-photon production in hadronic collisions [14–17], and also for jet production [12,18,19], which proceeds through the same partonic channels as inclusive-hadron production. We will actually make use of the results of [18,19] for the resummed jet cross section in our analysis below.

The larger  $\hat{x}_T$ , the more dominant the threshold logarithms will be. Since  $\hat{s} = x_1 x_2 S$ , where  $x_{1,2}$  are the partonic momentum fractions and  $\sqrt{S}$  is the hadronic c.m. energy, and since the parton distribution functions fall rapidly with increasing  $x_{1,2}$ , threshold effects become more and more relevant as the hadronic scaling variable  $x_T \equiv 2p_T/\sqrt{S}$  goes to one. This means that the fixed-target regime with  $3 \text{ GeV} \lesssim p_T \lesssim 10 \text{ GeV}$  and  $\sqrt{S}$  of 20–30 GeV is the place where threshold resummations are expected to be particularly relevant and useful. We will indeed confirm this in our study. Nonetheless, because of the convoluted form of the partonic cross sections and the parton distributions and fragmentation functions (see below), the threshold regime  $\hat{x}_T \rightarrow 1$  plays an important role also at much higher (collider) energies. Here one may, however, also have to pay attention to terms that are subleading near threshold.

In Sec. II we provide the basic formulas for the inclusive-hadron cross section at fixed order in perturbation theory, and display the role of the threshold region. Section III presents details of the threshold resummation for the inclusive-hadron cross section. In Sec. IV we give phenomenological results. We focus primarily on the fixed-target regime, but also give some exploratory results for collider energies. We do not present an exhaustive phenomenological analysis of all hadron production data available, but select some representative examples. Finally, we summarize our results in Sec. V. The appendix compiles some useful formulas for the threshold-resummed cross section.

## II. PERTURBATIVE CROSS SECTION AND THE THRESHOLD REGION

We consider single-inclusive hadron production in hadronic collisions,

$$H_1(P_1) + H_2(P_2) \rightarrow h(P_3) + X, \quad (1)$$

at large transverse momentum  $p_T$  of hadron  $h$ . We integrate over all angles (equivalently, pseudorapidities  $\eta$ ) of

the produced hadron. We note from the outset that this does not directly correspond to the experimental situation where always only a certain range in pseudorapidity is covered; we will return to this point later on. The factorized cross section for the process can then be written in terms of the convolution

$$\begin{aligned} \frac{p_T^3 d\sigma(x_T)}{dp_T} &= \sum_{a,b,c} \int_0^1 dx_1 f_{a/H_1}(x_1, \mu_{FI}^2) \\ &\times \int_0^1 dx_2 f_{b/H_2}(x_2, \mu_{FI}^2) \\ &\times \int_0^1 dz z^2 D_{h/c}(z, \mu_{FF}^2) \\ &\times \int_0^1 d\hat{x}_T \delta\left(\hat{x}_T - \frac{x_T}{z\sqrt{x_1 x_2}}\right) \\ &\times \int_{\hat{\eta}_-}^{\hat{\eta}_+} d\hat{\eta} \frac{\hat{x}_T^4 \hat{s}}{2} \frac{d\hat{\sigma}_{ab \rightarrow cX}(\hat{x}_T^2, \hat{\eta})}{d\hat{x}_T^2 d\hat{\eta}}, \quad (2) \end{aligned}$$

where  $\hat{\eta}$  is the pseudorapidity at parton level, with  $\hat{\eta}_+ = -\hat{\eta}_- = \ln[(1 + \sqrt{1 - \hat{x}_T^2})/\hat{x}_T]$ . The sum in Eq. (2) runs over all partonic subprocesses  $ab \rightarrow cX$ , with partonic cross sections  $d\hat{\sigma}_{ab \rightarrow cX}$ , parton distribution functions  $f_{a/H_1}$  and  $f_{b/H_2}$ , and parton-to-hadron fragmentation functions  $D_{h/c}$ . The scales  $\mu_{FI}$  and  $\mu_{FF}$  denote the factorization scales for the initial and final states, respectively. The dependence on them, and on the renormalization scale  $\mu_R$ , is implicit in the partonic cross section in Eq. (2).

The partonic cross sections are computed in QCD perturbation theory. Their expansions begin at  $\mathcal{O}(\alpha_s^2)$  since the LO partonic processes are the  $2 \rightarrow 2$  reactions  $ab \rightarrow cd$ . Therefore,

$$\begin{aligned} d\hat{\sigma}_{ab \rightarrow cX}(\hat{x}_T^2, \hat{\eta}) &= \alpha_s^2(\mu_R) [d\hat{\sigma}_{ab \rightarrow cd}^{(0)}(\hat{x}_T^2, \hat{\eta}) \\ &+ \alpha_s(\mu_R) d\hat{\sigma}_{ab \rightarrow cX}^{(1)}(\hat{x}_T^2, \hat{\eta}) + \mathcal{O}(\alpha_s^2)]. \quad (3) \end{aligned}$$

It is customary to express  $\hat{x}_T^2$  and  $\hat{\eta}$  in terms of a different set of variables,  $v$  and  $w$ :

$$\hat{x}_T^2 = 4vw(1-v), \quad e^{2\hat{\eta}} = \frac{vw}{1-v}. \quad (4)$$

At LO, one then has

$$\frac{\hat{s} d\hat{\sigma}_{ab \rightarrow cd}^{(0)}(v, w)}{dv dw} = \frac{\hat{s} d\hat{\sigma}_{ab \rightarrow cd}^{(0)}(v)}{dv} \delta(1-w), \quad (5)$$

where the  $\delta(1-w)$  function simply expresses the fact that  $\hat{x}_T \cosh(\hat{\eta}) \equiv 1$  for  $2 \rightarrow 2$  kinematics. It allows us to trivially perform the  $\hat{\eta}$  integration of the partonic cross section. Defining

$$\Sigma_{ab \rightarrow cX}(\hat{x}_T^2) \equiv \int_{\hat{\eta}_-}^{\hat{\eta}_+} d\hat{\eta} \frac{\hat{x}_T^4 \hat{s}}{2} \frac{d\hat{\sigma}_{ab \rightarrow cX}(\hat{x}_T^2, \hat{\eta})}{d\hat{x}_T^2 d\hat{\eta}}, \quad (6)$$

the LO cross section for the process  $gg \rightarrow gg$  becomes, for example,

$$\Sigma_{gg \rightarrow gg}^{(0)}(\hat{x}_T^2) = 18\alpha_S^2 \pi \frac{(1 - \frac{\hat{x}_T^2}{4})^3}{\sqrt{1 - \hat{x}_T^2}}. \quad (7)$$

Analytical expressions for the NLO corrections  $d\hat{\sigma}_{ab \rightarrow cX}^{(1)}(v, w)$  have been obtained in [2,4]. Schematically, they read:

$$\frac{\hat{s} d\hat{\sigma}_{ab \rightarrow cX}^{(1)}(v, w)}{dv dw} = A(v)\delta(1-w) + B(v)\left(\frac{\ln(1-w)}{1-w}\right)_+ + C(v)\left(\frac{1}{1-w}\right)_+ + F(v, w), \quad (8)$$

where the  $+$  distributions are defined in the usual way,

$$\int_0^1 f(w)[g(w)]_+ dw = \int_0^1 [f(w) - f(1)]g(w)dw. \quad (9)$$

The function  $F(w, v)$  in Eq. (8) represents all remaining terms without distributions in  $w$ . The terms with  $+$  distributions in Eq. (8) generate at NLO level the large logarithmic contributions we discussed earlier, and which we will resum to all orders in  $\alpha_S$ . After integration over  $\hat{\eta}$ , the term  $[\ln(1-w)/(1-w)]_+$  yields a contribution  $\propto \ln^2(1 - \hat{x}_T^2)$  to  $\Sigma_{ab \rightarrow cX}^{(1)}$ , plus terms less singular at  $\hat{x}_T = 1$ . At higher orders, the leading logarithmic contributions are enhanced by terms proportional to  $\alpha_S^k [\ln^{2k-1}(1-w)/(1-w)]_+$  in  $d\hat{\sigma}_{ab \rightarrow cX}^{(k)}(v, w)/dv dw$ , or to  $\alpha_S^k \ln^{2k}(1 - \hat{x}_T^2)$  in  $\Sigma_{ab \rightarrow cX}^{(k)}$ . As we discussed earlier, these logarithmic terms are due to soft-gluon radiation and, because there are two additional powers of the logarithm for each new order in perturbation theory, may spoil the perturbative expansion unless they are resummed to all orders.

As follows from Eq. (2), since the hadronic variable  $x_T$  is fixed,  $\hat{x}_T$  assumes particularly large values when the partonic momentum fractions approach the lower ends of their ranges. Since the parton distributions and fragmentation functions rise steeply towards small argument, this generally increases the relevance of the threshold regime and the soft-gluon effects are relevant even for situations where the hadronic center-of-mass energy is much larger than the transverse momentum of the final-state hadrons. This effect, valid in general in hadronic collisions, is even enhanced in single-inclusive hadron production since only a fraction  $z$  of the available energy is actually used to produce the final-state hadron.

### III. RESUMMED CROSS SECTION

We will now present the formulas for the threshold-resummed partonic cross sections. We will do this only for the case of the fully rapidity-integrated cross section, which turns out to significantly simplify the analysis. The

resummation for the  $\eta$  dependence of the kinematically related prompt-photon cross section was performed in Ref. [17], and we could in principle follow the techniques developed there to derive the  $\eta$  dependence of the resummed inclusive-hadron cross section. However, this process is of much greater complexity than prompt photons, as will become evident below, and it appears that a successful resummation at fixed rapidity will require further new techniques. We hope to address this in a future publication. As far as phenomenology is concerned, we will later on mimic the effects of the experimentally covered limited rapidity ranges by rescaling our resummed prediction by an appropriate ratio of NLO cross sections. Such an approximation was shown in [17] to work extremely well for the resummed prompt-photon cross section, where it was found that the shape of the cross section as a function of rapidity does not change much when going from NLO to the resummed result. This gives confidence that it may be applicable also in the case of inclusive-hadron production we are interested in.

#### A. Mellin moments and threshold region

The resummation of the soft-gluon contributions is carried out in Mellin- $N$  moment space, where the convolutions in Eq. (2) between parton distributions, fragmentation functions, and subprocess cross sections factorize into ordinary products. We take Mellin moments in the scaling variable  $x_T^2$  as

$$\sigma(N) \equiv \int_0^1 dx_T^2 (x_T^2)^{N-1} \frac{p_T^3 d\sigma(x_T)}{dp_T}. \quad (10)$$

In  $N$ -space Eq. (2) becomes

$$\sigma(N) = \sum_{a,b,c} f_{a/H_1}(N+1, \mu_{\text{FI}}^2) f_{b/H_2}(N+1, \mu_{\text{FI}}^2) \times D_{h/c}(2N+3, \mu_{\text{FF}}^2) \hat{\sigma}_{ab \rightarrow cX}(N), \quad (11)$$

with the Mellin moments of the parton distribution functions and fragmentation functions, and where

$$\begin{aligned} \hat{\sigma}_{ab \rightarrow cX}(N) &\equiv \int_0^1 d\hat{x}_T^2 (\hat{x}_T^2)^{N-1} \Sigma_{ab \rightarrow cX}(\hat{x}_T^2) \\ &= \frac{1}{2} \int_0^1 dw \int_0^1 dv [4v(1-v)w]^{N+1} \\ &\quad \times \frac{\hat{s} d\hat{\sigma}_{ab \rightarrow cX}^{(1)}(w, v)}{dw dv}. \end{aligned} \quad (12)$$

Here, the threshold limit  $w \rightarrow 1$  (or, for the rapidity-integrated cross section,  $\hat{x}_T^2 \rightarrow 1$ ) corresponds to  $N \rightarrow \infty$ , and the leading soft-gluon corrections arise as terms  $\propto \alpha_S^k \ln^{2k} N$ .

It is instructive to examine the interplay of rapidity integration and large- $N$  limit, for example, in case of the NLO cross section in Eq. (8). As we mentioned earlier, the

soft-gluon terms are associated with the  $+$  distribution pieces in (8), which have coefficients that may be written as functions of  $v$  only. One has

$$\int_0^1 dv [4v(1-v)w]^{N+1} f(v) = \int_0^1 dv [4v(1-v)w]^{N+1} \times \left[ f\left(\frac{1}{2}\right) + \mathcal{O}\left(\frac{1}{N}\right) \right], \quad (13)$$

which implies that at large  $N$  the variable  $v$  is ‘‘squeezed’’ to  $v = 1/2$ , and hence, as follows from (4), the partonic rapidity is forced to  $\hat{\eta} = 0$ . This means, for example, that near threshold it is justified to take the NLO partonic cross sections as proportional to the Born cross section,

$$\frac{\hat{s}d\hat{\sigma}_{ab \rightarrow cX}^{(1)}(v, w)}{dv dw} \approx \frac{\hat{s}d\hat{\sigma}_{ab \rightarrow cd}^{(0)}(v)}{dv} \left[ A' \delta(1-w) + B' \left( \frac{\ln(1-w)}{1-w} \right)_+ + C' \left( \frac{1}{1-w} \right)_+ \right], \quad (14)$$

with coefficients  $A', B', C'$  evaluated at  $v = 1/2$ . We will follow this reasoning also for the resummed cross section to which we turn now.

### B. Resummation to NLL

In Mellin-moment space, threshold resummation results in exponentiation of the soft-gluon corrections. Foremost, there are radiative factors for the initial and final partons, which contain the leading logarithms. At variance with the color-singlet cases of Drell-Yan and Higgs production [11,20,21], and with prompt-photon production [14,15] which has only one color structure at Born level, several color channels contribute to each of the  $2 \rightarrow 2$  QCD subprocesses relevant for inclusive-hadron production. As a result, there are color interferences and correlations in large-angle soft-gluon emission at NLL, and the resummed cross section for each subprocess becomes a sum of exponentials, rather than a single one.

In determining the resummed formula, we are in the fortunate situation that the effects of the color interferences for soft-gluon emission in the  $2 \rightarrow 2$  processes  $ab \rightarrow cd$  have been worked out in detail in Refs. [18,19] for the case of jet production in hadronic collisions, which proceeds through the same Born processes. We take advantage of the formulas derived there. The results in [18,19] have actually been given for arbitrary rapidity; for the case of the rapidity-integrated cross section we consider here it is sufficient to set  $\hat{\eta} = 0$  in the expressions of [18,19] when diagonalizing (by changing the color basis) the soft anomalous dimension matrix computed there. A difference between inclusive hadrons and jets occurs regarding the treatment of the final-state parton  $c$  producing the jet or the hadron. In our case, this parton is ‘‘observed,’’ that is,

we are considering a single-inclusive parton cross section. Such a cross section has final-state collinear singularities which are factorized into the fragmentation functions. As far as resummation is concerned, the final-state observed parton therefore is similar to the initial-state partons and receives essentially the same radiative factor as the latter [22].

Combining these results of [11,18,19,22], we can cast the resummed partonic cross section for each subprocess into the rather simple form

$$\hat{\sigma}_{ab \rightarrow cd}^{(\text{res})}(N-1) = C_{ab \rightarrow cd} \Delta_N^a \Delta_N^b \Delta_N^c J_N^d \times \left[ \sum_I G_{ab \rightarrow cd}^I \Delta_{IN}^{(\text{int})ab \rightarrow cd} \right] \hat{\sigma}_{ab \rightarrow cd}^{(\text{Born})}(N-1), \quad (15)$$

where the sum runs over all possible color configurations  $I$ , with  $G_{ab \rightarrow cd}^I$  representing a weight for each color configuration, such that  $\sum_I G_{ab \rightarrow cd}^I = 1$ .  $\hat{\sigma}_{ab \rightarrow cd}^{(\text{Born})}(N)$  denotes the  $N$ -moment expression for the Born cross section for the process, as defined in Eq. (12). We list the moment space expressions for all the Born cross sections in the appendix. Each of the functions  $\Delta_N^i, J_N^d, \Delta_{IN}^{(\text{int})ab \rightarrow cd}$  in Eq. (15) is an exponential.  $\Delta_N^a$  represents the effects of soft-gluon radiation collinear to initial parton  $a$  and is given, in the  $\overline{\text{MS}}$  scheme, by

$$\ln \Delta_N^a = \int_0^1 \frac{z^{N-1} - 1}{1-z} \int_{\mu_{FI}^2}^{(1-z)^2 Q^2} \frac{dq^2}{q^2} A_a(\alpha_S(q^2)), \quad (16)$$

and similarly for  $\Delta_N^b$ . Collinear soft-gluon radiation to parton  $c$  yields the same function, but with the initial-state factorization scale  $\mu_{FI}$  replaced with the final-state one,  $\mu_{FF}$ . The function  $J_N^d$  embodies collinear, soft or hard, emission by the nonobserved parton  $d$  and reads:

$$\ln J_N^d = \int_0^1 \frac{z^{N-1} - 1}{1-z} \left[ \int_{(1-z)^2 Q^2}^{(1-z)Q^2} \frac{dq^2}{q^2} A_d(\alpha_S(q^2)) + \frac{1}{2} B_d(\alpha_S(1-z)Q^2) \right]. \quad (17)$$

Large-angle soft-gluon emission is accounted for by the factors  $\Delta_{IN}^{(\text{int})ab \rightarrow cd}$ , which depend on the color configuration  $I$  of the participating partons. Each of the  $\Delta_{IN}^{(\text{int})ab \rightarrow cd}$  is given as

$$\ln \Delta_{IN}^{(\text{int})ab \rightarrow cd} = \int_0^1 \frac{z^{N-1} - 1}{1-z} D_{Iab \rightarrow cd}(\alpha_S((1-z)^2 Q^2)). \quad (18)$$

Finally, the coefficient  $C_{ab \rightarrow cd}$  contains  $N$ -independent hard contributions arising from one-loop virtual corrections.

In the above formulas, Eqs. (16)–(18), we have defined  $Q^2 = 2p_T^2$ . Furthermore, each of the functions  $\mathcal{F} \equiv A_a, B_a, D_{lab \rightarrow cd}$  is a perturbative series in  $\alpha_S$ ,

$$\mathcal{F}(\alpha_S) = \frac{\alpha_S}{\pi} \mathcal{F}^{(1)} + \left(\frac{\alpha_S}{\pi}\right)^2 \mathcal{F}^{(2)} + \dots, \quad (19)$$

with [23]:

$$A_a^{(1)} = C_a, A_a^{(2)} = \frac{1}{2} C_a \left[ C_A \left( \frac{67}{18} - \frac{\pi^2}{6} \right) - \frac{5}{9} N_f \right], \quad B_a^{(1)} = \gamma_a, \quad (20)$$

where  $N_f$  is the number of flavors, and

$$\begin{aligned} C_g &= C_A = N_c = 3, \\ C_q &= C_F = (N_c^2 - 1)/2N_c = 4/3, \\ \gamma_q &= -3C_F/2 = -2, \quad \gamma_g = -2\pi b_0, \\ b_0 &= \frac{1}{12\pi} (11C_A - 2N_f). \end{aligned} \quad (21)$$

The expansion of the coefficients  $C_{ab \rightarrow cd}$  reads:

$$C_{ab \rightarrow cd} = 1 + \frac{\alpha_S}{\pi} C_{ab \rightarrow cd}^{(1)} + \mathcal{O}(\alpha_S^2). \quad (22)$$

In the exponents, the large logarithms in  $N$  now occur only as single logarithms, of the form  $\alpha_S^k \ln^{k+1}(N)$  for the leading terms. Subleading terms are down by one or more powers of  $\ln(N)$ . Knowledge of the coefficients  $A_a^{(1,2)}, B_a^{(1)}, D_{lab \rightarrow cd}^{(1)}$  allows us to resum the full towers of leading logarithms (LL)  $\alpha_S^k \ln^{k+1}(N)$ , and NLL  $\alpha_S^k \ln^k(N)$  in the exponent. Along with the coefficients  $C_{ab \rightarrow cd}^{(1)}$  one then gains control of three towers of logarithms in the cross section,  $\alpha_S^k \ln^{2k}(N)$ ,  $\alpha_S^k \ln^{2k-1}(N)$ ,  $\alpha_S^k \ln^{2k-2}(N)$ , which is likely to lead to a much improved theoretical prediction. We also note that the factors  $\Delta_N^i$  depend on the initial- or final-state factorization scales in such a way that they will compensate the scale dependence (evolution) of the parton distribution and fragmentation functions. One therefore expects a decrease in scale dependence, which indeed has been found in previous studies for other threshold-resummed cross sections.

We finally examine the qualitative impact of the resummation. To this end, we note that, neglecting the running of the strong coupling, the LL terms in the exponents in Eqs. (16) and (17) become

$$\begin{aligned} \Delta_N^a &= \exp \left[ \frac{\alpha_S}{\pi} C_a \ln^2(N) \right], \\ J_N^d &= \exp \left[ -\frac{\alpha_S}{2\pi} C_d \ln^2(N) \right]. \end{aligned} \quad (23)$$

Therefore, for each partonic channel, the leading logarithms are

$$\hat{\sigma}_{ab \rightarrow cd}^{(\text{res})}(N) \propto \exp \left[ \frac{\alpha_S}{\pi} \left( C_a + C_b + C_c - \frac{1}{2} C_d \right) \ln^2(N) \right]. \quad (24)$$

The fact that this exponent is clearly positive for each of the partonic channels means that the soft-gluon effects will lead to an enhancement of the cross section. Particularly strong enhancements are to be expected for gluonic channels; for example, for the process  $gg \rightarrow gg$  one has  $C_a + C_b + C_c - C_d/2 = 15/2$ . The feature that partonic cross sections can give Sudakov enhancements is related to the fact that finite partonic cross sections are obtained after collinear (mass) factorization, so that soft-gluon effects are partly already contained in the ( $\overline{\text{MS}}$ -defined) parton distribution functions and, in our case, fragmentation functions.

### C. Exponents at NLL

We now give explicit formulas for the expansions of the resummed exponents to NLL accuracy. Since the functions  $\Delta_N^i$  and  $J_N^d$  are “universal” in the sense that they depend only on the type of the external parton, but not on the subprocess, their expansions are known and we recall them for the sake of completeness:

$$\begin{aligned} \ln \Delta_N^a(\alpha_S(\mu_R^2), Q^2/\mu_R^2; Q^2/\mu_F^2) \\ = \ln N h_a^{(1)}(\lambda) + h_a^{(2)}(\lambda, Q^2/\mu_R^2; Q^2/\mu_F^2) \\ + \mathcal{O}(\alpha_S(\alpha_S \ln N)^k), \end{aligned} \quad (25)$$

$$\begin{aligned} \ln J_N^d(\alpha_S(\mu_R^2), Q^2/\mu_R^2) = \ln N f_d^{(1)}(\lambda) + f_d^{(2)}(\lambda, Q^2/\mu_R^2) \\ + \mathcal{O}(\alpha_S(\alpha_S \ln N)^k), \end{aligned} \quad (26)$$

where  $\lambda = b_0 \alpha_S(\mu_R^2) \ln N$ . The functions  $h^{(1,2)}$  and  $f^{(1,2)}$  are given by

$$h_a^{(1)}(\lambda) = \frac{A_a^{(1)}}{2\pi b_0 \lambda} [2\lambda + (1 - 2\lambda) \ln(1 - 2\lambda)], \quad (27)$$

$$\begin{aligned} h_a^{(2)}(\lambda, Q^2/\mu_R^2; Q^2/\mu_F^2) = -\frac{A_a^{(2)}}{2\pi^2 b_0^2} [2\lambda + \ln(1 - 2\lambda)] - \frac{A_a^{(1)} \gamma_E}{\pi b_0} \ln(1 - 2\lambda) + \frac{A_a^{(1)} b_1}{2\pi b_0^3} \left[ 2\lambda + \ln(1 - 2\lambda) + \frac{1}{2} \ln^2(1 - 2\lambda) \right] \\ + \frac{A_a^{(1)}}{2\pi b_0} [2\lambda + \ln(1 - 2\lambda)] \ln \frac{Q^2}{\mu_R^2} - \frac{A_a^{(1)}}{\pi b_0} \lambda \ln \frac{Q^2}{\mu_F^2}, \end{aligned} \quad (28)$$

$$f_d^{(1)}(\lambda) = -\frac{A_d^{(1)}}{2\pi b_0 \lambda} [(1 - 2\lambda) \ln(1 - 2\lambda) - 2(1 - \lambda) \ln(1 - \lambda)], \quad (29)$$

$$\begin{aligned}
f_a^{(2)}(\lambda, Q^2/\mu_R^2) = & -\frac{A_a^{(1)}b_1}{2\pi b_0^3} \left[ \ln(1-2\lambda) - 2\ln(1-\lambda) + \frac{1}{2}\ln^2(1-2\lambda) - \ln^2(1-\lambda) \right] \\
& + \frac{B_a^{(1)}}{2\pi b_0} \ln(1-\lambda) - \frac{A_a^{(1)}\gamma_E}{\pi b_0} [\ln(1-\lambda) - \ln(1-2\lambda)] - \frac{A_a^{(2)}}{2\pi^2 b_0^2} [2\ln(1-\lambda) - \ln(1-2\lambda)] \\
& + \frac{A_a^{(1)}}{2\pi b_0} [2\ln(1-\lambda) - \ln(1-2\lambda)] \ln \frac{Q^2}{\mu_R^2}. \tag{30}
\end{aligned}$$

Here, as before  $b_0 = (11C_A - 2N_f)/12\pi$ , and

$$b_1 = \frac{1}{24\pi^2} (17C_A^2 - 5C_A N_f - 3C_F N_f). \tag{31}$$

We remind the reader that the scale  $\mu_F$  represents the initial-state (final-state) factorization scale  $\mu_{FI}$  ( $\mu_{FF}$ ) for the radiative factors for the initial (final) state. The functions  $h^{(1)}$  and  $f^{(1)}$  above contain all LL terms in the perturbative series, while  $h^{(2)}$  and  $f^{(2)}$  are of NLL accuracy only. For a complete NLL resummation one also needs the coefficients  $\ln\Delta_{IN}^{(\text{int})ab\rightarrow cd}$  whose NLL expansion reads:

$$\begin{aligned}
\ln\Delta_{IN}^{(\text{int})ab\rightarrow cd}(\alpha_S(\mu_R^2), Q^2/\mu_R^2) \\
= \frac{D_{Iab\rightarrow cd}^{(1)}}{2\pi b_0} \ln(1-2\lambda) + \mathcal{O}(\alpha_S(\alpha_S \ln N)^k). \tag{32}
\end{aligned}$$

As we mentioned earlier, the  $D_{Iab\rightarrow cd}^{(1)}$ , and the corresponding ‘‘color weights’’  $G_{Iab\rightarrow cd}$ , are both process and ‘‘color configuration’’ dependent. All the coefficients  $D_{Iab\rightarrow cd}^{(1)}$  and  $G_{Iab\rightarrow cd}$  that we need to NLL are listed in the appendix.

#### D. Coefficients $C_{ab\rightarrow cd}^{(1)}$

We have verified for each subprocess that expansion of the resummed formulas above to  $\mathcal{O}(\alpha_S^3)$  correctly reproduces the logarithmic terms  $\propto \alpha_S^3 \ln^2(N)$ ,  $\alpha_S^3 \ln(N)$  known from the full fixed-order calculations [2,4]. Comparison to those calculations also allows us to extract the first-order coefficients  $C_{ab\rightarrow cd}^{(1)}$ . Numerical results for the coefficients are presented in the appendix.

#### E. Matching to the NLO cross section, and inverse Mellin transform

As we have discussed above, the resummation is achieved in Mellin-moment space. In order to obtain a resummed cross section in  $x_T^2$  space, one needs an inverse Mellin transform. This requires a prescription for dealing with the singularity in the perturbative strong coupling constant in Eqs. (16)–(18) or in the NLL expansions, Eqs. (27)–(32). We will use the *Minimal Prescription* developed in Ref. [24], which relies on use of the NLL expanded forms Eqs. (27)–(32), and on choosing a Mellin contour in complex- $N$  space that lies to the *left* of the poles at  $\lambda = 1/2$  and  $\lambda = 1$  in the Mellin integrand:

$$\frac{p_T^3 d\sigma^{(\text{res})}(x_T)}{dp_T} = \int_{C_{MP}-i\infty}^{C_{MP}+i\infty} \frac{dN}{2\pi i} (x_T^2)^{-N} \sigma^{(\text{res})}(N), \tag{33}$$

where  $b_0\alpha_S(\mu_R^2)\ln C_{MP} < 1/2$ , but all other poles in the integrand are as usual to the left of the contour. The result defined by the minimal prescription has the property that its perturbative expansion is an asymptotic series that has no factorial divergence and therefore no ‘‘built-in’’ power-like ambiguities. Power corrections may then be added, as phenomenologically required.

When performing the resummation, one of course wants to make full use of the available fixed-order cross section, which in our case is NLO ( $\mathcal{O}(\alpha_S^3)$ ). Therefore, a matching to this cross section is appropriate, which may be achieved by expanding the resummed cross section to  $\mathcal{O}(\alpha_S^3)$ , subtracting the expanded result from the resummed one, and adding the full NLO cross section:

$$\begin{aligned}
\frac{p_T^3 d\sigma^{(\text{match})}(x_T)}{dp_T} = & \sum_{a,b,c} \int_{C_{MP}-i\infty}^{C_{MP}+i\infty} \frac{dN}{2\pi i} (x_T^2)^{-N+1} f_{a/h_1}(N, \mu_{FI}^2) f_{b/h_2}(N, \mu_{FI}^2) D_{c/h}(2N+1, \mu_{FF}^2) \\
& \times [\hat{\sigma}_{ab\rightarrow cd}^{(\text{res})}(N-1) - \hat{\sigma}_{ab\rightarrow cd}^{(\text{res})}(N-1)|_{\mathcal{O}(\alpha_S^3)}] + \frac{p_T^3 d\sigma^{(\text{NLO})}(x_T)}{dp_T}, \tag{34}
\end{aligned}$$

where  $\hat{\sigma}_{ab\rightarrow cd}^{(\text{res})}(N)$  is the resummed cross section for the partonic channel  $ab \rightarrow cd$  as given in Eq. (15). In this way, NLO is taken into account in full, and the soft-gluon contributions beyond NLO are resummed to NLL. Any double-counting of perturbative orders is avoided.

#### IV. PHENOMENOLOGICAL RESULTS

Starting from Eq. (34), we are now ready to present some first resummed results at the hadronic level. This is not meant to be an exhaustive study of the available data for inclusive-hadron production; rather we should like to

investigate the overall size and relevance of the resummation effects. We will only consider  $\pi^0$  production in  $pp$  collisions and compare to a few selected sets of data.

Let us begin by specifying some “default” choices for the distribution functions that we will use in our studies. We will use the MRST2002 set of parton densities [25] and the pion fragmentation functions of [26] (referred to as “KKP”). For comparison, we will also present some results for Kretzer’s set [27] of fragmentation functions. Note that, according to Eq. (34), it is a great advantage to have parton densities and fragmentation functions available in moment space. Technically, since the MRST distributions are not available in moment space, we first performed a fit of a simple functional form to the MRST distributions, of which we were then able to take moments. This had to be done separately for each parton type and for each scale. Concerning the fragmentation functions, Kretzer’s set is anyway set up in moment space, and we found it possible to analytically take moments of the KKP parametrization.

As we discussed at the end of subsection III B, we generally expect fairly large effects from soft-gluon resummation for inclusive-hadron production. This makes it rather important to be sure that the resummed soft-gluon terms indeed constitute the dominant part of the cross section and do not, for example, lead to an overestimate of the higher orders. We therefore start by identifying the kinematic regions where soft-gluon contributions are likely to dominate the cross section. A gauge for this is obtained

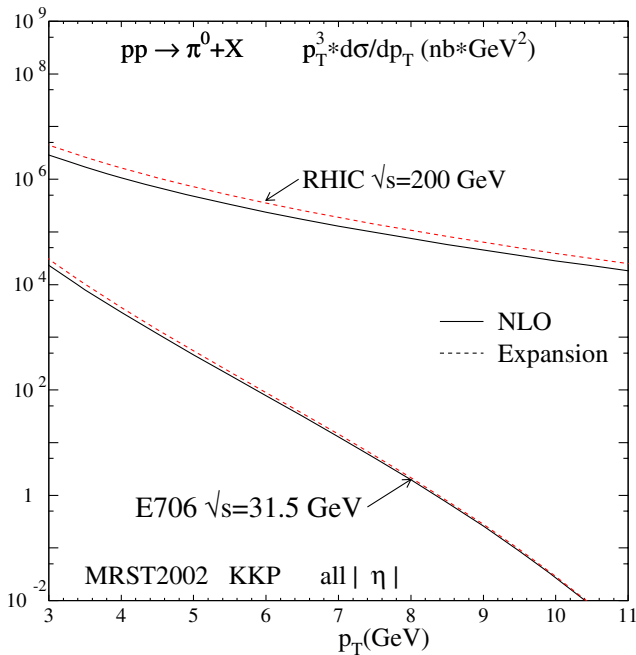


FIG. 1 (color online). Comparison of full NLO cross sections (solid lines) for  $pp \rightarrow \pi^0 X$  with the NLO [ $\mathcal{O}(\alpha_s^3)$ ] expansion of the resummed cross section (dashed lines), for two different energies. We have chosen the factorization and renormalization scales as  $p_T$ .

by comparing the resummed formula expanded to NLO to the full fixed-order (NLO) perturbative result, that is, by comparing the last two terms in Eq. (34). Figure 1 shows this comparison for a typical fixed-target energy  $\sqrt{s} = 31.5$  GeV, and for RHIC’s  $\sqrt{s} = 200$  GeV. As can be observed, the expansion faithfully reproduces the NLO result. In the fixed-target regime the agreement is excellent, except perhaps at the lowest pion transverse momenta,  $p_T \sim 3$  GeV, where the soft approximation tends to yield a slight overestimate. This is obviously related to the fact that the smaller  $p_T$  (at fixed energy), the further one is away from threshold, so that the soft-gluon approximations become less reliable. The same is expected to happen if the energy is increased at fixed transverse momentum. Indeed, as the curves for  $\sqrt{s} = 200$  GeV in Fig. 1 show, the NLO-expanded resummed result, while still remarkably close to the full NLO prediction, gives a less accurate picture of the latter than at fixed-target energies. Our conclusion from Fig. 1 is therefore that the contributions associated with the near-threshold region are dominant in the fixed-target regime, implying that resummation will be relevant and accurate here, even at relatively small transverse momenta. At colliders, our resummed cross section will likely be too large, and further improvements in the theoretical framework may be needed.<sup>1</sup> We will briefly return to this point at the end of this paper. In the following we will primarily focus on the fixed-target regime.

We next investigate how large the higher-order contributions provided by NLL resummation are. To this end, we go back to Eq. (34) and take the full resummed result, defined in the minimal prescription and matched to NLO. As before, the cross sections are integrated over all rapidities. We define a resummed “ $K$ -factor” as the ratio of the resummed cross section to the NLO cross section,

$$K^{(\text{res})} = \frac{d\sigma^{(\text{match})}/dp_T}{d\sigma^{(\text{NLO})}/dp_T}, \quad (35)$$

which is shown for the fixed-target regime, and for scales  $\mu_R = \mu_{\text{FI}} = \mu_{\text{FF}} = p_T$ , by the solid line in Fig. 2. As can be seen,  $K^{(\text{res})}$  is very large, meaning that resummation results in a dramatic enhancement over NLO. It is then interesting to see how this enhancement builds up order by order in the resummed cross section. We therefore expand the matched resummed formula beyond NLO and define the “soft-gluon  $K$ -factors”

$$K^n \equiv \frac{d\sigma^{(\text{match})}/dp_T|_{\mathcal{O}(\alpha_s^{2+n})}}{d\sigma^{(\text{NLO})}/dp_T}, \quad (36)$$

<sup>1</sup>It is worth recalling that our matching procedure given by Eq. (34) ensures that the NLO cross section is always fully and exactly taken into account in our final “matched” cross section, so that any overestimate would only occur at NNLO and beyond.

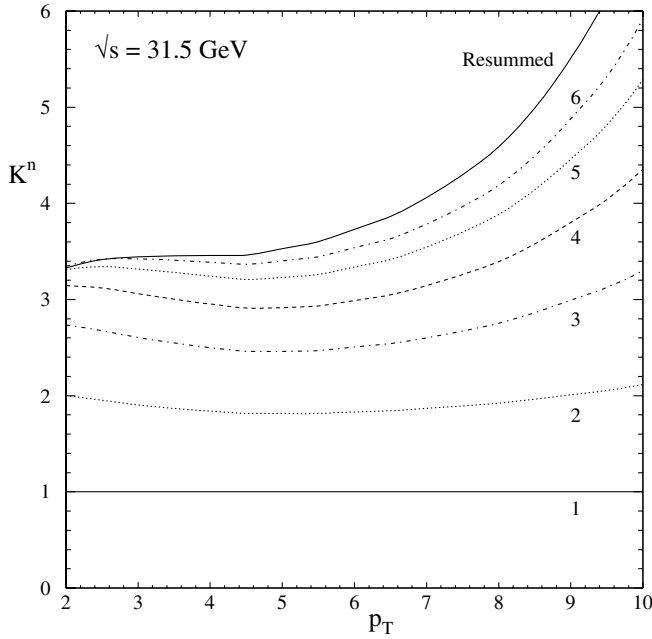


FIG. 2. “ $K$ -factors” relative to NLO as defined in Eqs. (35) and (36) for  $pp \rightarrow \pi^0 X$  in the fixed-target regime.

which for  $n = 2, 3, \dots$  give the additional enhancement over full NLO due to the  $\mathcal{O}(\alpha_s^{2+n})$  terms in the resummed formula. Formally,  $K^1 = 1$  and  $K^\infty = K^{(\text{res})}$  of Eq. (35). The results for  $K^{2,3,4,5,6}$  are also shown in Fig. 2. One can see that there are very large contributions even beyond NNLO, in particular, at the higher  $p_T$ . Clearly, the full resummation given by the solid line is required here.

As we have mentioned earlier, we have determined the resummed formulas for the fully rapidity-integrated cross section, whereas in experiment always only a certain limited range of rapidity is covered. In order to be able to compare to data, we therefore approximate the cross section in the experimentally accessible rapidity region by

$$\begin{aligned} & \frac{p_T^3 d\sigma^{(\text{match})}}{dp_T} (\eta \text{ in exp. range}) \\ &= K^{(\text{res})} \frac{p_T^3 d\sigma^{(\text{NLO})}}{dp_T} (\eta \text{ in exp. range}), \end{aligned} \quad (37)$$

where  $K^{(\text{res})}$  is as defined in Eq. (35) in terms of cross sections integrated over the full region of rapidity. In other words, we rescale the matched resummed result by the ratio of NLO cross sections integrated over the experimentally relevant rapidity region or over all  $\eta$ , respectively.

In Fig. 3 we compare the NLL resummed and NLO predictions to the available data from E706 [28] for  $pp \rightarrow \pi^0 X$  at  $\sqrt{S} = 31.5$  GeV. The data cover  $|\eta| < 0.75$ . We use the KKP fragmentation functions [26] and give results for three different choices of scales,  $\mu_R = \mu_{\text{FI}} = \mu_{\text{FF}} = \zeta p_T$ , where  $\zeta = 1/2, 1, 2$ . It is evident that the NLO result falls far short of the data, which is an observation that has

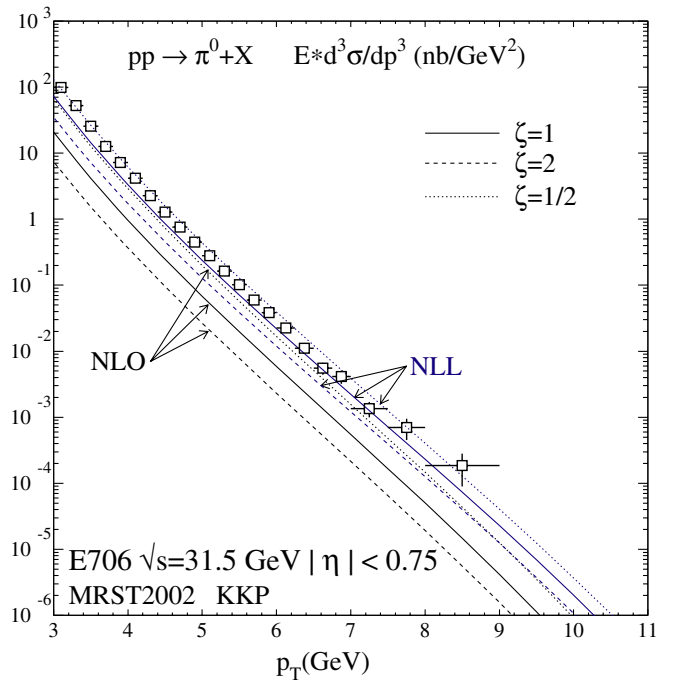


FIG. 3 (color online). NLO and NLL resummed results for the cross section for  $pp \rightarrow \pi^0 X$  for E706 kinematics. We have used the KKP fragmentation functions [26]. Results are given for three different choices of scales,  $\mu_R = \mu_{\text{FI}} = \mu_{\text{FF}} = \zeta p_T$ , where  $\zeta = 1/2, 1, 2$ . Data are from [28].

been made before [5–7]. Furthermore, there is a very large scale dependence at NLO. The situation is significantly improved when the NLL resummation is taken into account. As we already saw in Fig. 2, the NLL matched cross section is considerably higher than the NLO one, and it shows a markedly improved comparison to the E706 data, probably satisfactory in view of the overall uncertainties. Furthermore, the scale dependence is considerably reduced compared to the NLO calculation, and hence the accuracy of the prediction is improved.

Figure 4 shows the same result, but now for the Kretzer set [27] of pion fragmentation functions. These functions are known to be overall significantly smaller than the ones of KKP, in particular, for the gluon fragmentation function which is not well determined from the  $e^+e^- \rightarrow hX$  data.<sup>2</sup> One therefore finds that all theory curves are shifted downward with respect to the results shown in the previous figure. Nevertheless, the effects due to threshold resummation remain large.

To give another example, Fig. 5 presents a comparison to data from the WA70 experiment, corresponding to

<sup>2</sup>Note that analyses of hadron production in the additional jet in  $e^+e^- \rightarrow b\bar{b}$ jet events [29] do constrain  $D_g^\pi$  significantly. The  $D_g^\pi$ 's in the sets of [26,27] are in reasonable agreement with these data, with the one of [27] arguably setting a lower bound on  $D_g^\pi$ .



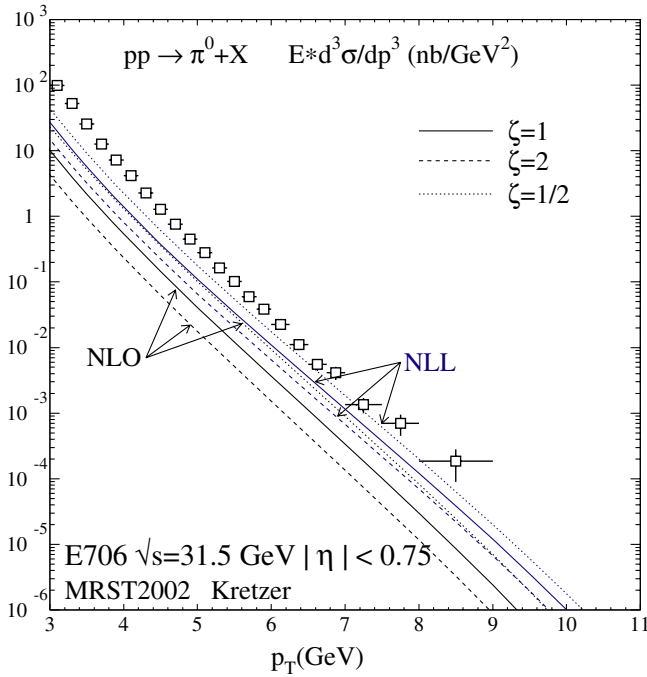


FIG. 4 (color online). Same as Fig. 3, but for the set of fragmentation functions of [27].

$\sqrt{S} = 31.5$  GeV and  $|x_F| < 0.45$ . Again a significant enhancement due to NLL resummation is found, resulting in a much improved agreement between theory and data.

Finally, in Fig. 6 we repeat the calculations for the case of proton-proton collisions at RHIC with  $\sqrt{S} = 200$  GeV

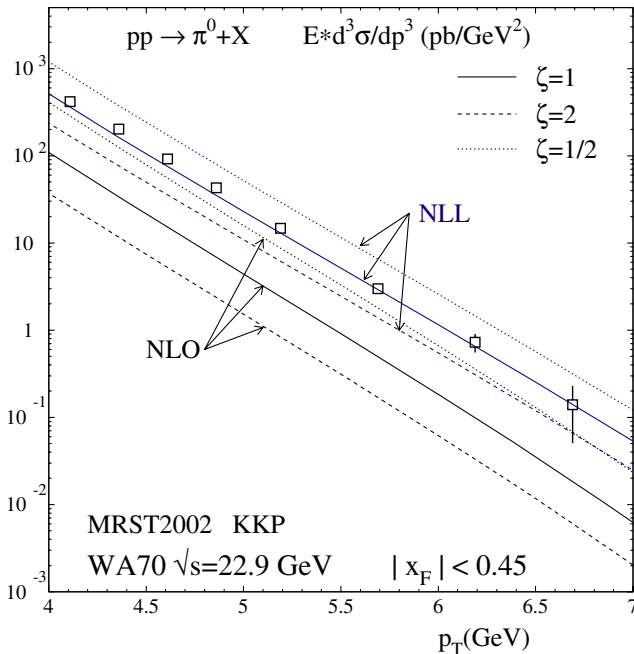


FIG. 5 (color online). Same as Fig. 3, but comparing to the  $pp \rightarrow \pi^0 X$  data of WA70 [35] at  $\sqrt{S} = 22.9$  GeV.

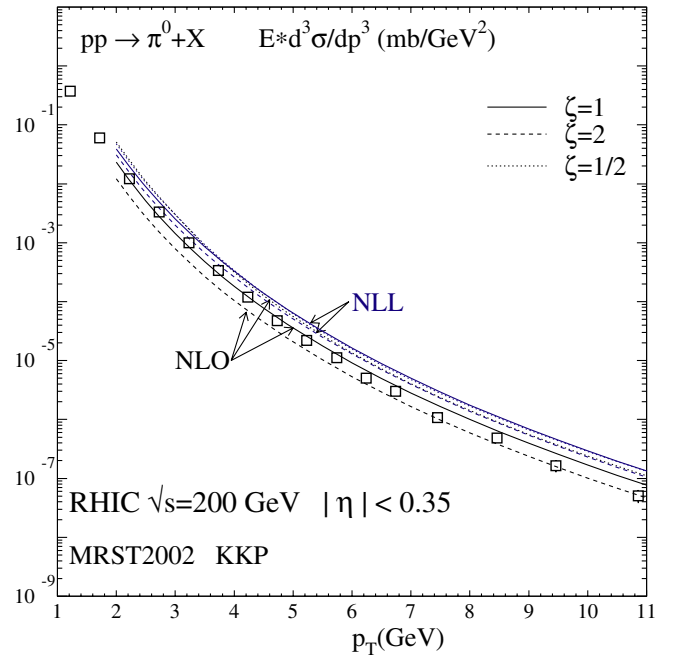


FIG. 6 (color online). Same as Fig. 3, but comparing to the RHIC PHENIX data of [9].

and  $|\eta| < 0.35$ . The data are from the measurement performed by the PHENIX Collaboration [9]. Again, an enhancement from resummation is found which, however, is smaller than in the previous figures. This is expected since we are further away from threshold here, due to the much higher energy. Nevertheless, the enhancement is quite significant at the larger  $p_T$ , where in fact the resummed result appears to lie too high. We emphasize, however, that according to our results shown in Fig. 1 it is likely that the NLL resummation gives an overestimate of the higher-order corrections in this case. We therefore do not take the enhancement too literally and reserve its closer investigation to a future study. We note that also in this case there is a considerable reduction in the scale dependence, and that again the fragmentation functions of [27] lead to a smaller cross section.

## V. CONCLUSIONS AND OUTLOOK

We have studied the NLL all-order resummation of threshold logarithms in the partonic cross sections relevant for the process  $pp \rightarrow hX$  at high transverse momentum of the hadron  $h$ . This study has in part been motivated by the observed shortfall of fixed-order (NLO) cross sections when compared to experimental data in the fixed-target regime, in contrast with the excellent agreement of data and theory at colliders. Our numerical results indeed show a strong enhancement of the cross section over the next-to-leading order one for typical fixed-target kinematics, significantly improving the agreement between data and theoretical predictions. At higher energies, such as at

RHIC, the resummation effects are less important, but more theoretical analysis is needed here due to the likely relevance of subleading terms.

We emphasize that the contributions generated by resummation are a well-defined class of higher-order corrections to the leading-power partonic cross sections that will be present in the full perturbative series order by order and actually dominate it. Our results are then also to be seen in the context of the size of possible nonperturbative power-suppressed corrections to the cross section. Any residual shortfall of the resummed theoretical prediction would need to be attributed to such contributions. In previous studies, “intrinsic” transverse momenta of partons have often been taken into account in (LO or NLO) calculations of inclusive-hadron cross sections [6,30], in order to bridge the large gaps between data and NLO theory in the fixed-target regime. These can perhaps best be viewed as models of the power-suppressed contributions. In light of our results, however, much of the enhancements needed for a satisfactory description of the fixed-target data appears to come from perturbative contributions, so that power-suppressed contributions are probably of rather moderate size. It is interesting to note that resummed perturbation theory itself may provide information on the structure of power corrections, through ambiguities in the perturbative series [31] arising from the pole in the perturbative running coupling in the expressions Eqs. (16)–(18). A recent study [32] addressed this issue in the case of single-inclusive cross sections at large  $x_T$  and indeed estimated power corrections to be not very sizable. On the other hand, it is known [15–17] that threshold resummation effects are not very large for the prompt photon cross section in the fixed-target regime, where discrepancies between data and NLO theory of similar magnitude as for pion production have been observed in some cases. This issue clearly needs further study.

We finally emphasize that we regard this study only as the beginning of a more detailed analysis of threshold resummation for inclusive-hadron cross sections. There are several points in which further developments are desirable. First of all, as we noted earlier, it would be possible in principle (albeit challenging technically) to perform the resummation correctly for the fully rapidity-dependent cross section. To do this appears all the more interesting since it was observed [7] that the discrepancies between

NLO and fixed-target data actually increase (at fixed  $p_T$ ) toward larger rapidities. We expect resummation effects to become even more important as well at large  $\eta$ , simply because one is approaching threshold more closely. It is also possible to improve the resummation by resumming also terms of the form  $\alpha_S^k \ln^{2k-1}(N)/N$  in the partonic cross sections. Such terms arise from collinear emissions [20,21,33]; they are suppressed with respect to the LL and NLL terms but may nonetheless be of relevance if one is further away from threshold as, for example, in the fixed-target regime at lower  $p_T$ , or a collider energies. We expect that such additional contributions would also further decrease the scale dependence. With these improvements in place, detailed phenomenological studies of power corrections might become possible. We finally also note that another important field for further study would be the effects of threshold resummation on spin asymmetries, in particular, on the double-longitudinal spin asymmetries  $A_{LL}$  measured by E704 [34] and at RHIC [9]. We believe that the significant enhancements due to resummation that we found in this work strongly motivate all these further studies.

## ACKNOWLEDGMENTS

We are grateful to S. Catani and G. Sterman for a careful reading of the manuscript, and to S. Kretzer for useful discussions. The work of D.dF has been partially supported by Conicet, Fundación Antorchas, UBACyT and ANPCyT. W.V. is grateful to RIKEN, Brookhaven National Laboratory and the U.S. Department of Energy (Contract No. DE-AC02-98CH10886) for providing the facilities essential for the completion of his work.

## APPENDIX: RESULTS FOR THE VARIOUS SUBPROCESSES

In this appendix we compile the moment-space expressions for the Born cross sections for the various partonic subprocesses, and the process dependent coefficients  $C_{ab \rightarrow cd}^{(1)}$ ,  $D_{Iab \rightarrow cd}$ , and  $G_{ab \rightarrow cd}^I$ . Since the  $C_{ab \rightarrow cd}^{(1)}$  have rather lengthy expressions, we only give their numerical values for  $N_f = 5$  and the factorization and renormalization scales set to  $\mu_{FI} = \mu_{FF} = \mu_R = Q$ .

$qq' \rightarrow qq'$ :

$$\begin{aligned} \hat{\sigma}_{qq' \rightarrow qq'}^{(\text{Born})}(N) &= \frac{\pi C_F}{3C_A} (5N^2 + 15N + 12) B\left(N, \frac{5}{2}\right), \\ G_{1qq' \rightarrow qq'} &= 1/3, \quad G_{2qq' \rightarrow qq'} = 2/3, \quad D_{1qq' \rightarrow qq'}^{(1)} = -4 \ln 2, \quad D_{2qq' \rightarrow qq'}^{(1)} = 0, \\ C_{1qq' \rightarrow qq'}^{(1)} &= 20.2389 \quad (N_f = 5). \end{aligned} \tag{A1}$$

$q\bar{q}' \rightarrow q\bar{q}'$ :

$$\hat{\sigma}_{q\bar{q}' \rightarrow q\bar{q}'}^{(\text{Born})}(N) = \frac{\pi C_F}{3C_A}(5N^2 + 15N + 12)B\left(N, \frac{5}{2}\right),$$

$$G_{1q\bar{q}' \rightarrow q\bar{q}'} = 1/9, \quad G_{2q\bar{q}' \rightarrow q\bar{q}'} = 8/9, \quad D_{1q\bar{q}' \rightarrow q\bar{q}'}^{(1)} = -10/3 \ln 2, \quad D_{2q\bar{q}' \rightarrow q\bar{q}'}^{(1)} = 8/3 \ln 2, \quad (\text{A2})$$

$$C_{1q\bar{q}' \rightarrow q\bar{q}'}^{(1)} = 22.4483 \quad (N_f = 5).$$

$q\bar{q} \rightarrow q'\bar{q}'$ :

$$\hat{\sigma}_{q\bar{q} \rightarrow q'\bar{q}'}^{(\text{Born})}(N) = \frac{\pi C_F}{6C_A}(N+1)(N+3)B\left(N+1, \frac{5}{2}\right),$$

$$G_{1q\bar{q} \rightarrow q'\bar{q}'} = 1, \quad D_{1q\bar{q} \rightarrow q'\bar{q}'}^{(1)} = -10/3 \ln 2, \quad C_{1q\bar{q} \rightarrow q'\bar{q}'}^{(1)} = 7.91881 \quad (N_f = 5). \quad (\text{A3})$$

$qq \rightarrow qq$ :

$$\hat{\sigma}_{qq \rightarrow qq}^{(\text{Born})}(N) = \frac{2\pi C_F}{3C_A^2}(C_A(5N^2 + 15N + 12) - 2N(3 + 2N))B\left(N, \frac{5}{2}\right),$$

$$G_{1qq \rightarrow qq} = 9/11, \quad G_{2qq \rightarrow qq} = 2/11, \quad D_{1qq \rightarrow qq}^{(1)} = -4 \ln 2, \quad D_{2qq \rightarrow qq}^{(1)} = 0, \quad (\text{A4})$$

$$C_{1qq \rightarrow qq}^{(1)} = 19.535 \quad (N_f = 5).$$

$q\bar{q} \rightarrow q\bar{q}$ :

$$\hat{\sigma}_{q\bar{q} \rightarrow q\bar{q}}^{(\text{Born})}(N) = \frac{\pi C_F}{15C_A^2}(C_A(11N^3 + 59N^2 + 102N + 60) + N(N+3)(5+2N))B\left(N, \frac{7}{2}\right),$$

$$G_{1q\bar{q} \rightarrow q\bar{q}} = 5/21, \quad G_{2q\bar{q} \rightarrow q\bar{q}} = 16/21, \quad D_{1q\bar{q} \rightarrow q\bar{q}}^{(1)} = -10/3 \ln 2, \quad D_{2q\bar{q} \rightarrow q\bar{q}}^{(1)} = 8/3 \ln 2, \quad (\text{A5})$$

$$C_{1q\bar{q} \rightarrow q\bar{q}}^{(1)} = 19.9643 \quad (N_f = 5).$$

$q\bar{q} \rightarrow gg$ :

$$\hat{\sigma}_{q\bar{q} \rightarrow gg}^{(\text{Born})}(N) = \frac{\pi C_F}{3C_A}(2C_F(N+2)(5+2N) - C_A(N+1)(N+3))B\left(N+1, \frac{5}{2}\right),$$

$$G_{1q\bar{q} \rightarrow gg} = 5/7, \quad G_{2q\bar{q} \rightarrow gg} = 2/7, \quad D_{1q\bar{q} \rightarrow gg}^{(1)} = -10/3 \ln 2, \quad D_{2q\bar{q} \rightarrow gg}^{(1)} = 8/3 \ln 2, \quad (\text{A6})$$

$$C_{1q\bar{q} \rightarrow gg}^{(1)} = 12.4329 \quad (N_f = 5).$$

$qg \rightarrow qg$ :

$$\hat{\sigma}_{qg \rightarrow qg}^{(\text{Born})}(N) = \frac{\pi}{6C_A}(C_F N(7+5N) + 2C_A(5N^2 + 15N + 12))B\left(N, \frac{5}{2}\right),$$

$$G_{1qg \rightarrow qg} = 45/88, \quad G_{2qg \rightarrow qg} = 25/88, \quad G_{3qg \rightarrow qg} = 18/88, \quad D_{1qg \rightarrow qg}^{(1)} = -14/3 \ln 2, \quad (\text{A7})$$

$$D_{2qg \rightarrow qg}^{(1)} = 10/3 \ln 2, \quad D_{3qg \rightarrow qg}^{(1)} = -2/3 \ln 2, \quad C_{1qg \rightarrow qg}^{(1)} = 15.4167 \quad (N_f = 5).$$

$qg \rightarrow gq$ :

$$\hat{\sigma}_{qg \rightarrow gq}^{(\text{Born})}(N) = \frac{\pi}{6C_A}(C_F N(7+5N) + 2C_A(5N^2 + 15N + 12))B\left(N, \frac{5}{2}\right),$$

$$G_{1qg \rightarrow gq} = 45/88, \quad G_{2qg \rightarrow gq} = 25/88, \quad G_{3qg \rightarrow gq} = 18/88, \quad D_{1qg \rightarrow gq}^{(1)} = -8 \ln 2, \quad (\text{A8})$$

$$D_{2qg \rightarrow gq}^{(1)} = 0, \quad D_{3qg \rightarrow gq}^{(1)} = -4 \ln 2, \quad C_{1qg \rightarrow gq}^{(1)} = 22.4474 \quad (N_f = 5).$$

$gg \rightarrow gg$ :

$$\hat{\sigma}_{gg \rightarrow gg}^{(\text{Born})}(N) = \frac{\pi C_A}{5C_F}(9N^3 + 45N^2 + 72N + 40)B\left(N, \frac{7}{2}\right),$$

$$G_{1gg \rightarrow gg} = 1/3, \quad G_{2gg \rightarrow gg} = 1/2, \quad G_{3gg \rightarrow gg} = 1/6, \quad D_{1gg \rightarrow gg}^{(1)} = 0, \quad (\text{A9})$$

$$D_{2gg \rightarrow gg}^{(1)} = -10 \ln 2, \quad D_{3gg \rightarrow gg}^{(1)} = 6 \ln 2, \quad C_{1gg \rightarrow gg}^{(1)} = 21.1977 \quad (N_f = 5).$$

$gg \rightarrow q\bar{q}$ :

$$\hat{\sigma}_{gg \rightarrow q\bar{q}}^{(\text{Born})}(N) = \frac{\pi}{12C_A C_F} (2C_F(N+2)(5+2N) - C_A(N+1)(N+3)) B\left(N+1, \frac{5}{2}\right),$$

$$G_{1gg \rightarrow q\bar{q}} = 5/7, \quad G_{2gg \rightarrow q\bar{q}} = 2/7, \quad D_{1gg \rightarrow q\bar{q}}^{(1)} = 0, \quad D_{2gg \rightarrow q\bar{q}}^{(1)} = 6 \ln 2, \quad (\text{A10})$$

$$C_{1gg \rightarrow q\bar{q}}^{(1)} = 16.7962 \quad (N_f = 5).$$

In the above expressions,  $B(a, b)$  is the Beta-function.

- 
- [1] B. L. Combridge, J. Kripfganz, and J. Ranft, Phys. Lett. **70B**, 234 (1977); J. F. Owens, E. Reya, and M. Glück, Phys. Rev. D **18**, 1501 (1978).
- [2] F. Aversa, P. Chiappetta, M. Greco, and J. P. Guillet, Nucl. Phys. **B327**, 105 (1989).
- [3] D. de Florian, Phys. Rev. D **67**, 054004 (2003).
- [4] B. Jäger, A. Schäfer, M. Stratmann, and W. Vogelsang, Phys. Rev. D **67**, 054005 (2003).
- [5] P. Aurenche, M. Fontannaz, J. P. Guillet, B. A. Kniehl, and M. Werlen, Eur. Phys. J. C **13**, 347 (2000).
- [6] U. Baur *et al.*, hep-ph/0005226.
- [7] C. Bourrely and J. Soffer, Eur. Phys. J. C **36**, 371 (2004).
- [8] B. A. Kniehl, G. Kramer, and B. Potter, Nucl. Phys. **B597**, 337 (2001).
- [9] S. S. Adler *et al.* (PHENIX Collaboration), Phys. Rev. Lett. **91**, 241803 (2003).
- [10] J. Adams *et al.* (STAR Collaboration), Phys. Rev. Lett. **92**, 171801 (2004).
- [11] G. Sterman, Nucl. Phys. **B281**, 310 (1987); S. Catani and L. Trentadue, Nucl. Phys. **B327**, 323 (1989); **B353**, 183 (1991).
- [12] N. Kidonakis and G. Sterman, Nucl. Phys. **B505**, 321 (1997).
- [13] R. Bonciani, S. Catani, M. L. Mangano, and P. Nason, Phys. Lett. B **575**, 268 (2003).
- [14] E. Laenen, G. Oderda, and G. Sterman, Phys. Lett. B **438**, 173 (1998).
- [15] S. Catani, M. L. Mangano, and P. Nason, J. High Energy Phys. 07 (1998) 024; S. Catani, M. L. Mangano, P. Nason, C. Oleari, and W. Vogelsang, J. High Energy Phys. 03 (1999) 025.
- [16] N. Kidonakis and J. F. Owens, Phys. Rev. D **61**, 094004 (2000).
- [17] G. Sterman and W. Vogelsang, J. High Energy Phys. 02 (2001) 016.
- [18] N. Kidonakis, G. Oderda, and G. Sterman, Nucl. Phys. **B525**, 299 (1998); **B531**, 365 (1998).
- [19] N. Kidonakis and J. F. Owens, Phys. Rev. D **63**, 054019 (2001).
- [20] M. Krämer, E. Laenen, and M. Spira, Nucl. Phys. **B511**, 523 (1998).
- [21] S. Catani, D. de Florian, M. Grazzini, and P. Nason, J. High Energy Phys. 07 (2003) 028.
- [22] M. Cacciari and S. Catani, Nucl. Phys. **B617**, 253 (2001).
- [23] J. Kodaira and L. Trentadue, Phys. Lett. **112B**, 66 (1982); Phys. Lett. B **123**, 335 (1983); S. Catani, E. D’Emilio, and L. Trentadue, Phys. Lett. B **211**, 335 (1988).
- [24] S. Catani, M. L. Mangano, P. Nason, and L. Trentadue, Nucl. Phys. **B478**, 273 (1996).
- [25] A. D. Martin, R. G. Roberts, W. J. Stirling, and R. S. Thorne, Eur. Phys. J. C **28**, 455 (2003).
- [26] B. A. Kniehl, G. Kramer, and B. Potter, Nucl. Phys. **B582**, 514 (2000).
- [27] S. Kretzer, Phys. Rev. D **62**, 054001 (2000).
- [28] L. Apanasevich *et al.* (Fermilab E706 Collaboration), Phys. Rev. D **68**, 052001 (2003).
- [29] See, e.g.: P. Abreu *et al.* (DELPHI Collaboration), Eur. Phys. J. C **13**, 573 (2000), and references therein.
- [30] A. P. Contogouris, R. Gaskell, and S. Papadopoulos, Phys. Rev. D **17**, 2314 (1978); L. Apanasevich *et al.*, Phys. Rev. D **59**, 074007 (1999); U. D’Alesio and F. Murgia, Phys. Rev. D **70**, 074009 (2004).
- [31] G. ’t Hooft, Nucl. Phys. **B138**, 1 (1978); A. H. Mueller, Nucl. Phys. **B250**, 327 (1985); M. Beneke and V. M. Braun, in *At the Frontier of Particle Physics/Handbook of QCD*, edited by M. Shifman (World Scientific, Singapore, 2001), and references therein; M. Beneke and V. M. Braun, Nucl. Phys. **B454**, 253 (1995); Y. L. Dokshitzer, G. Marchesini, and B. R. Webber, Nucl. Phys. **B469**, 93 (1996); J. High Energy Phys. 07 (1999) 012; G. P. Korchemsky and G. Sterman, Nucl. Phys. **B437**, 415 (1995); R. Akhoury and V. I. Zakharov, Phys. Lett. B **357**, 646 (1995); Nucl. Phys. **B465**, 295 (1996); Phys. Rev. Lett. **76**, 2238 (1996); G. Sterman and W. Vogelsang, hep-ph/9910371.
- [32] G. Sterman and W. Vogelsang, Phys. Rev. D **71**, 014013 (2005).
- [33] A. Kulesza, G. Sterman, and W. Vogelsang, Phys. Rev. D **66**, 014011 (2002).
- [34] D. L. Adams *et al.* (E581 Collaboration), Phys. Lett. B **261**, 197 (1991); D. L. Adams *et al.* (FNAL E581/704 Collaboration), Phys. Lett. B **336**, 269 (1994).
- [35] M. Bonesini *et al.* (WA70 Collaboration), Z. Phys. C **38**, 371 (1988).